ELSEVIER

Journal of Biomechanics 38 (2005) 305–314

JOURNAL OF BIOMECHANICS

www.elsevier.com/locate/jbiomech
www.JBiomech.com

Computational wear prediction of a total knee replacement from in vivo kinematics

Benjamin J. Fregly[a,b,c,*], W. Gregory Sawyer[a], Melinda K. Harman[d], Scott A. Banks[a,c,d]

[a] *Department of Mechanical & Aerospace Engineering, University of Florida, Gainesville, FL 32611, USA*
[b] *Department of Biomedical Engineering, University of Florida, Gainesville, FL, USA*
[c] *Department of Orthopaedics and Rehabilitation, University of Florida, Gainesville, FL, USA*
[d] *Orthopaedic Research Laboratory, The Biomotion Foundation, West Palm Beach, FL 33401, USA*

Abstract

Wear of ultra-high molecular weight polyethylene bearings in total knee replacements remains a major limitation to the longevity of these clinically successful devices. Few design tools are currently available to predict mild wear in implants based on varying kinematics, loads, and material properties. This paper reports the implementation of a computer modeling approach that uses fluoroscopically measured motions as inputs and predicts patient-specific implant damage using computationally efficient dynamic contact and tribological analyses. Multibody dynamic simulations of two activities (gait and stair) with two loading conditions (70–30 and 50–50 medial–lateral load splits) were generated from fluoroscopic data to predict contact pressure and slip velocity time histories for individual elements on the tibial insert surface. These time histories were used in a computational wear analysis to predict the depth of damage due to wear and creep experienced by each element. Predicted damage areas, volumes, and maximum depths were evaluated against a tibial insert retrieved from the same patient who provided the in vivo motions. Overall, the predicted damage was in close agreement with damage observed on the retrieval. The gait and stair simulations separately predicted the correct location of maximum damage on the lateral side, whereas a combination of gait and stair was required to predict the correct location on the medial side. Predicted maximum damage depths were consistent with the retrieval as well. Total computation time for each damage prediction was less than 30 min. Continuing refinement of this approach will provide a robust tool for accurately predicting clinically relevant wear in total knee replacements.
© 2004 Elsevier Ltd. All rights reserved.

Keywords: Computational wear prediction; Dynamic contact simulation; Patient-specific modeling

1. Introduction

Wear of ultra-high molecular weight polyethylene (UHMWPE) in total knee replacements remains a major limitation to the longevity of these clinically successful devices (Peters et al., 1992; Cadambi et al., 1994; Jacobs et al., 1994; Sharkey et al., 2002). Improvements over the past decade in sterilization techniques have reduced oxidative degradation of the UHMWPE bearing, with potentially dramatic long-term reductions in fatigue-related pitting and delamination wear (Li and Burstein, 1994; Williams et al., 1998). However, abrasive-adhesive wear mechanisms remain, with the potential to generate large numbers of submicron debris particles of osteolytic potential (Lewis, 1997; Ezzet et al., 1995; Jacobs et al., 2002). Efforts to reduce abrasive-adhesive or "mild" wear have resulted in the introduction of more highly crosslinked polymer bearings (McKellop et al., 1999; Wroblewski et al., 1999; Crossfire™, Durasul™, Longevity™, and Marathon™—see Appendix for web sites) and more scratch-resistant, highly wettable femoral articular surfaces (Walker et al., 1996; Heimke et al., 2002; Oxinium™ and zirconia ceramic—see Appendix for web sites). These technologies may reduce, but cannot eliminate, mild wear mechanisms.

Because mild wear is a function of contact pressure, material properties, and kinematics (Blunn et al., 1991; Wimmer and Andriacchi, 1997; Sathasivam and Walker, 1998; Wimmer et al., 1998; Harman et al., 2001), efforts to minimize it must necessarily address these three determinants. Unfortunately, the relationships between contact pressure, kinematics, and wear have been poorly

*Corresponding author. Department of Mechanical and Aerospace Engineering, University of Florida, 231 MAE-A Building, P.O. Box 116250, Gainesville, FL 32611-6250, USA. Tel.: +1-352-392-8157; fax: +1-352-392-7303.
E-mail address: fregly@ufl.edu (B.J. Fregly).

0021-9290/$ - see front matter © 2004 Elsevier Ltd. All rights reserved.
doi:10.1016/j.jbiomech.2004.02.013

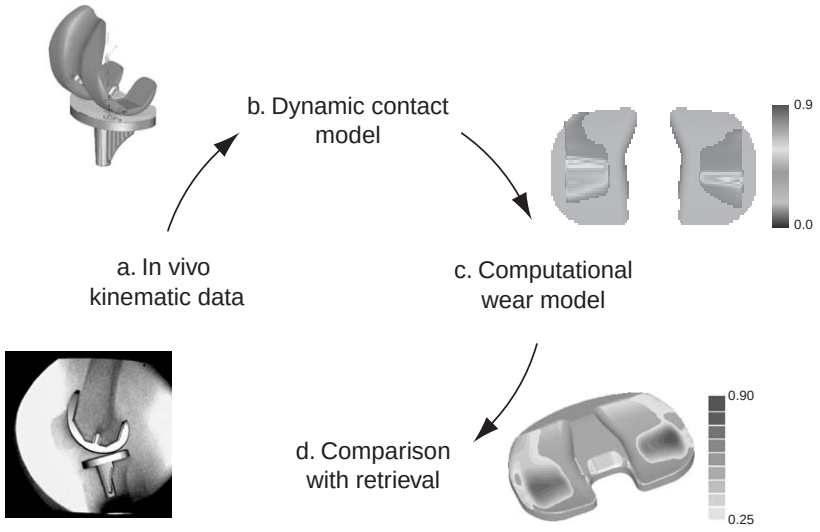

Fig. 1. Overview of the experimental and computer modeling methods used to develop and evaluate wear predictions. (a) In vivo fluoroscopic data provide patient-specific kinematic inputs to a dynamic contact model of the same knee design and size; (b) the dynamic model predicts contact pressures and slip velocities experienced by individual elements on the tibial insert surface and outputs these data to a computational wear model; (c) the wear model performs wear and creep analyses to calculate the total damage depth for each element and outputs the worn geometry to computer-aided inspection software; and (d) the inspection software produces color contour maps of the predicted damage regions, which are compared with a damage contour map produced from a laser scan of the tibial insert retrieved from the same patient whose fluoroscopic data were used as model inputs.

understood for implant-scale systems, making prediction of clinical wear performance a historically daunting challenge. Recent advances in computational mechanics, tribology, and in vivo assessment might now provide the required tools to permit accurate prediction of clinical implant wear performance.

The goal of the present effort was to demonstrate the feasibility of combining in vivo measurement of knee kinematics (Fig. 1a), computation of the resulting dynamic contact pressures (Fig 1b), and tribological modeling (Fig 1c) to accurately predict clinical wear in a patient-specific model. The effort was guided by the concept that no tuning of model parameters would be done, and only previously published values for material properties and other input parameters would be used. Predicted damage was compared to the autopsy-retrieved tibial insert from the same patient whose in vivo kinematics were used as model inputs (Fig. 1d). Despite uncertain parameters and simplified modeling methods, the proposed computational wear methodology is able to capture many of the significant characteristics observed upon retrieval.

2. Materials and methods

2.1. In vivo kinematic data

Fluoroscopic kinematic data previously collected from one total knee arthroplasty patient (female, age 65 at time of surgery, height 170 cm, mass 70 kg) were used in this study (Harman et al., 2001). The patient received a cemented posterior cruciate ligament retaining prosthesis (Series 7000, Stryker Howmedica Osteonics, Inc., Allendale, NJ) with a 6.8 mm thick insert machined from slab molded polyethylene sheets sterilized with gamma radiation in air. The insert geometry was essentially flat in the sagittal and coronal planes, with slight dishing at the anterior and posterior borders. The multiradius femoral component had three separate sagittal plane radii. The angle created by the femoral and tibial shaft axes was 172° and the tibial component alignment in the sagittal plane was 90° on post-operative radiographs (Ewald, 1989). Knee Society Clinical Rating System (Insall et al., 1989) scores were 97 (knee) and 80 (function) after 1 year and 99 (knee) and 100 (function) after 2 years. The patient gave written informed consent to participate in the kinematic and retrieval studies as previously described (Harman et al., 2001).

The patient performed treadmill gait and stair rise/descent activities during fluoroscopic motion analysis (Banks, 1992; Banks and Hodge, 1996; Banks et al., 1997a, b) 21 months after surgery (Fig. 1a). This analysis method matches three-dimensional computer-aided design (CAD) models of the prosthetic components provided by the manufacturer to the two-dimensional fluoroscopic images and is accurate to approximately 1° for all rotations and 0.5 mm for translations in the sagittal plane (Banks and Hodge, 1996). Kinematic data from one representative cycle of each activity were averaged in 5° increments of knee flexion for stair and

1% increments for gait including stance and swing phases. The duration of the cycle was 1.22 s for gait and 4.6 s for stair.

2.2. Dynamic contact model

A multibody dynamic contact model was constructed from the same implant CAD model used in the fluoroscopic motion analysis. A commercial software program (Pro/MECHANICA MOTION, Parametric Technology Corporation, Waltham, MA) provided the multibody dynamics framework, and an elastic contact model was integrated into this framework using user-supplied routines (Fig. 1b; Fregly et al., 2003). The contact model utilized elastic foundation theory (Johnson, 1985; An et al., 1990; Blankevoort et al., 1991; Li et al., 1997) which scatters a "bed of springs" over the three-dimensional surfaces to push them apart. The springs represent an elastic layer of known thickness covering one or both bodies, where each spring is independent from its neighbors. For a rigid femur contacting a deformable tibial insert of finite thickness, the contact pressure p for any spring can be calculated from (Johnson, 1985; An et al., 1990; Blankevoort et al., 1991)

$$p = \frac{(1-v)E}{(1+v)(1-2v)h}d, \tag{1}$$

where E is Young's modulus of the elastic layer, v is Poisson's ratio of the layer, h is the layer thickness at the spring location, and d is the spring deflection, defined as the interpenetration of the undeformed surfaces in the direction of the local surface normal. E was chosen to be 463 MPa (Kurtz et al., 2002) corresponding to gamma radiation crosslinked virgin GUR 1050 polyethylene and v was chosen as 0.46 (Bartel et al., 1995). All geometry calculations were performed using the ACIS 3D Toolkit (Spatial Corporation, Westminster, CO). The original CAD geometry in the regions of contact was re-surfaced using Geomagic Studio (Raindrop Geomagic, Research Triangle Park, NC) to eliminate potential problems caused by seams between surface patches. The tolerance between the original and re-surfaced geometry was ± 0.002 mm. No faceting of the geometry was required for the contact calculations.

The dynamic contact model used in vivo fluoroscopic measurements (anterior–posterior translation, internal–external rotation, and flexion; Figs. 2a–c, respectively) as prescribed kinematic inputs. The model predicted the remaining degrees of freedom (axial translation, varus–valgus rotation, and medial–lateral translation) via forward dynamic simulation to ensure compatibility with the applied loads (see below). All prescribed and predicted motions were for the femur moving with respect to a fixed tibia.

Four loads applied to the femoral component affected the predicted motions. The first was an axial force applied vertically downward and positioned to produce either a 70–30 or 50–50 medial–lateral load split at 0° flexion (Johnson et al., 1981; Schipplein and Andriacchi, 1991; Hurwitz et al., 1998). With two activities (gait and stair) and two load splits (70–30 and 50–50), this produced four cases for dynamic simulation. The axial force curve for each activity was defined by scaling the vertical ground reaction force curve to be between 0.25 and 3.0 BW (Fig. 2d; Schipplein and Andriacchi, 1991; Lu et al., 1997; Taylor et al., 1998; Taylor and Walker, 2001). Ground reaction force data were not available from the fluoroscopy/retrieval patient, so vertical forces during gait and stair activities from a patient of similar age, height, weight, and knee flexion characteristics were used (Banks et al., 2000). The stance phase of the gait force data was extended from 62% to 68% of the cycle to match the treadmill kinematics. The second load was a medial–lateral nonlinear spring force of the form $k(ax)^b$, where $k = 100$, $a = 2$, and $b = 4$, which produces a small restoring force in the region $|x| \leqslant 0.5$ mm and ramps up quickly for $|x| > 0.5$ mm. This force was included to prevent the femoral component from "riding" the medial eminence of the tibial insert in the 70–30 load split simulations and had little effect on the 50–50 simulations. The third load was comprised of the net force and torque due to elastic contact in the medial and lateral tibiofemoral compartments. The final load was comprised of the inertial force and torque, which was made negligible by choosing small values for the femoral component mass and inertia.

The dynamic contact model generated wear model inputs in two steps. A forward dynamics simulation with a coarse contact element grid was used to predict accurate contact forces and kinematics, since the contact forces and torques were highly insensitive to grid density. A subsequent inverse dynamics analysis with a finer element grid was used to predict accurate contact pressures and slip velocities from these kinematics, since the peak and average contact pressures are much more sensitive to grid density. Though accurate kinematics and contact pressures could be predicted simultaneously, this two-stage approach minimized CPU time. To determine the necessary resolution of the coarse grid, the predicted contact forces and torques were investigated using the lightest load (0.25 BW) and smallest contact area (90° flexion). For a fixed static configuration, convergence to within 3% relative error occurred for a 35×20 grid on each side. The accuracy of the dynamic simulation results produced with this grid was verified by repeating the simulations using a denser 50×35 grid. With the coarse 35×20 grid, each forward dynamics simulation required between 10 and 15 min of CPU time on a 2.4 GHz Pentium IV workstation, while the finer 50×35 grid required between 18 and 21 min of

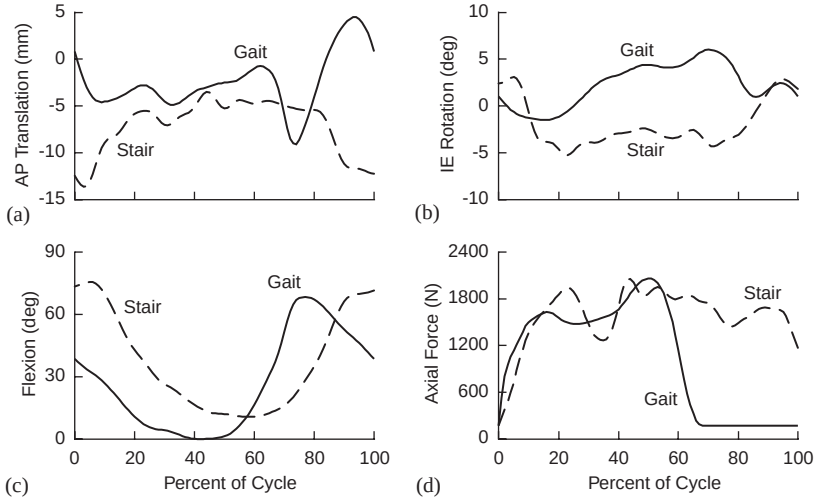

Fig. 2. In vivo experimental data used as inputs to the dynamic contact model: (a) Anterior–posterior (AP) translation; (b) internal–external (IE) rotation; (c) Flexion; and (d) axial force. Kinematic data are from pre-retrieval video fluoroscopy gait and stair experiments with the femur moving with respect to the tibia. Anterior translation and external rotation are positive. Axial force data are scaled vertical ground reaction force data from a patient of similar age, height, weight, and knee flexion characteristics.

CPU time. The subsequent inverse dynamics analysis used a 50×50 element grid (see Fig. 5) and required less than 2 min of CPU time for each case.

2.3. Computational wear model

A computational wear model was developed to produce element-by-element damage predictions given the predicted time history of contact pressures and slip velocities experienced by each element. The model computes total damage depth for each element as the sum of material removal due to mild wear and surface deformation due to compressive creep:

$$\delta_{\text{Damage}} = N\delta_{\text{Wear}} + \delta_{\text{Creep}}, \tag{2}$$

where δ_{Damage} is the total damage, δ_{Wear} is the damage per cycle due to mild wear, N is the total number of cycles, and δ_{Creep} is the damage due to creep. N was calculated from the number of months of implantation (see below) assuming 1 million cycles per year of gait or stair (Schmalzried et al., 1998).

The depth of material removed from an element over one cycle due to mild wear was predicted using Archard's classic wear law (Archard and Hirst, 1956):

$$\delta_{\text{Wear}} = k\sum_{i=1}^{n} p_i d_i = k\sum_{i=1}^{n} p_i |v_i|\,\Delta t, \tag{3}$$

where k is the material wear rate, i is a discrete time instant in an activity measured at n instants, p_i is the contact pressure on the element at that instant, and d_i is the sliding distance experienced by the element, calculated as the product of slip velocity magnitude $|v_i|$ at that instant and increment Δt between time instants. To determine an appropriate value of k, the articulating surface of the retrieved metal femoral component was examined under a white-light optical interferometer (Wyko NT1000, Veeco Instruments, Woodbury, NY). The average roughness R_a measured at multiple locations on the contact surfaces varied between 46 and 275 nm with a mean value of 131 nm. Published wear rates as a function of R_a were examined for UHMWPE of similar age to that implanted in the patient and subjected to similar contact pressure, slip velocity, and environmental conditions (Fisher et al., 1994). Since the reported wear rates vary dramatically with R_a, the average value of R_a was used to select an average wear rate of $k = 220 \times 10^{-9}\ \text{mm}^3/\text{N m}$.

Because UHMWPE is a viscoelastic material that deforms in a time-dependent manner under load (Waldman and Bryant, 1994, 1997; Lee and Pienkowski, 1998), not all surface profile changes in retrieved components are a result of wear. Experiments to determine the compressive creep characteristics of medical grade extruded UHMWPE were performed by Lee and Pienkowski (1998). Their results can be formulated into the following equation for the depth of element surface deformation due to creep over the total time of implantation:

$$\delta_{\text{Creep}} = \left[3.491 \times 10^{-3} + 7.996 \times 10^{-4}\left(\text{Log}\left(N\sum_{i=1}^{n}\Delta t_{ci}\right) - 4\right)\right]\frac{\sum_{i=1}^{n} p_{ci}\,\Delta t_{ci}}{\sum_{i=1}^{n}\Delta t_{ci}}\,h, \tag{4}$$

where all notations are as defined previously with the exceptions that the subscript c denotes use of only those time instants i when the contact pressure p_i is non-zero, h is the minimum thickness of the tibial insert, the unit for pressure must be MPa, the unit for time minutes,

and the unit for thickness mm. Since no data were found in the literature that could be used to form a creep recovery equation similar to Eq. (4), zero relaxation was assumed rather than estimating a relaxation percentage that could not be justified. Thus, the predicted values of δ_{Creep} will be overestimates.

Implanted components see a wide spectrum of activities depending on the age and lifestyle of the patient, with different activities placing different tribological demands on the joint. To account for the varying spectrum of activities, a linear damage model (linear rules-of-mixture) was used to predict the total damage δ_{Damage} produced by any combination of gait δ_{Gait} and stair δ_{Stair} activities. With the fraction of each activity denoted by x_{Gait} and x_{Stair} for gait and stair, respectively, where $x_{Gait} + x_{Stair} = 1$, the total damage depth for any assumed partitioning of activities is given by

$$\delta_{Damage} = x_{Gait}\delta_{Gait} + (1 - x_{Gait})\delta_{Stair}, \quad (5)$$

where δ_{Gait} and δ_{Stair} are computed from Eq. (2) assuming all cycles are either gait or stair.

2.4. Comparison with retrieval

Five computational wear predictions (two activities with two load splits, and one partition of activities: 85% gait and 15% stair) were compared to the actual damage depths and patterns measured on the tibial insert retrieved from the patient post-mortem. The total time of implantation at retrieval was 51 months. For both the predictions and the retrieval, visualizations of the wear contours were generated using commercial automatic inspection software (Geomagic Qualify, Raindrop Geomagic, Research Triangle Park, NC). For the wear predictions, the center of each contact element on the tibial insert surface was displaced by the calculated damage depth δ_{Damage} in the direction of the local surface normal. A "worn" polygonal surface model was created from these points, and a contour plot of the deviations between the original and worn surfaces was generated by the software.

The retrieval showed scratching, burnishing, and tractive striations on the articular surfaces (Harman et al., 2001). Pitting and delamination were not observed. A three-dimensional scan was obtained of the worn insert (Fig. 3a) and a matched unworn insert using a laser scanner (Vivid 900, Minolta Corporation, Ramsey, NJ) possessing a manufacturer-reported accuracy of ± 0.04 mm. Once the point clouds generated by the laser scans were converted to polygonal surface models and aligned by the software, a retrieval wear contour plot was also generated (Fig. 3b). To determine a threshold for reporting retrieval wear, the unworn insert was aligned with the insert CAD model and the maximum deviation between contact surfaces (0.25 mm) determined.

3. Results

Qualitatively, the damage regions predicted by the computer simulations were in good agreement with the clinical damage regions (compare Fig. 4 with Fig. 3). The medial damage scars for the 70–30 gait case (Fig. 4a) extended to the anterior medial corner of the insert, similar to the retrieval. In contrast, the medial damage scars for the 70–30 (Fig. 4b) stair case extended broadly to the posterior rim of the insert, enlarging the region predicted by the gait cases. The lateral damage scars for the 70–30 gait case extended more anteriorly than in the retrieval, whereas the anterior border on the lateral side in the 70–30 stair case corresponded well with the retrieval. Altering the load split to 50–50 decreased medial damage while increasing lateral damage for both gait (Fig. 4c) and stair (not shown). For an 85% gait, 15% stair partitioning of activities based on linear rules of mixture, the damage area for a 70–30 load split (Fig. 4d) was a combination of the gait (Fig. 4a) and stair

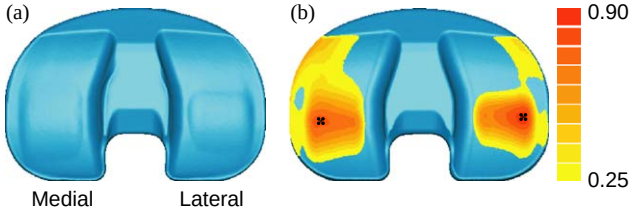

Fig. 3. Damage visualization of the retrieved tibial insert: (a) laser scan showing damage regions visible to the naked eye; and (b) contour map indicating depth of damage zones. Colorbar indicates depth in mm. Stars indicate location of maximum damage on each side.

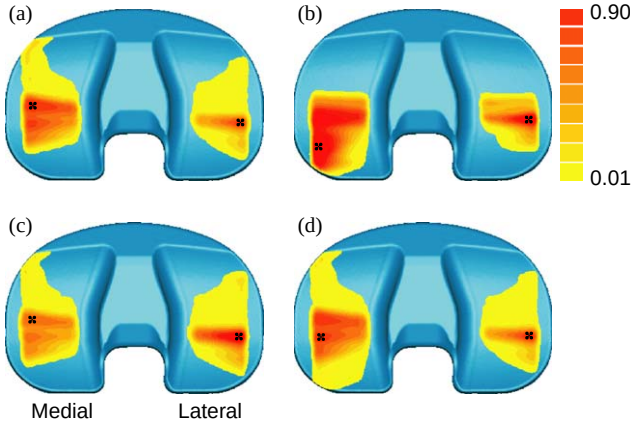

Fig. 4. Damage contour maps predicted by the computer simulations: (a) gait with 70–30 load split; (b) stair with 70–30 load split; (c) gait with 50–50 load split; and (d) combined activity assuming 85% gait, 15% stair with 70–30 load split. Colorbar indicates depth in mm. Stars indicate location of maximum damage on each side. Both gait and stair accurately predicted the location of maximum damage on the lateral side, while only combined activity predicted the correct location on the medial side.

Table 1
Quantitative summary of damage results predicted by the computer simulations for gait and stair activities with 70–30 and 50–50 load splits

Load split	Damage	Gait			Stair		
		Medial	Lateral	Total	Medial	Lateral	Total
70–30	Wear depth (mm)	0.5	0.5	—	0.6	0.7	—
	Creep depth (mm)	0.5	0.3	—	2.1	0.5	—
	Damage depth (mm)	1.0	0.8	—	2.7	1.2	—
	Area (mm^2)	372	321	693	337	206	543
	Damage volume (mm^3)	123	54	177	200	74	274
50–50	Wear depth (mm)	0.3	0.7	—	0.5	0.9	—
	Creep depth (mm)	0.4	0.4	—	0.6	0.7	—
	Damage depth (mm)	0.7	1.1	—	1.1	1.6	—
	Area (mm^2)	359	352	711	318	233	551
	Damage volume (mm^3)	94	85	179	147	113	260

Maximum wear, creep, and total damage may occur at different locations on the surface.

(Fig. 4b) damage areas. For both gait and stair, the lateral wear regions were more central in the anterior–posterior direction than were the medial regions, similar to the retrieval, and possessed a posterior border of similar shape and location to the retrieval.

The predicted locations of maximum damage were in good agreement with the retrieval (stars in Figs. 3b and 4). On the lateral side, the location of maximum damage was the same in all four simulations and was consistent with the retrieval. On the medial side, the maximum damage location was shifted anteriorly for the gait simulations (Figs. 4a and c) and posteriorly for the stair simulations (Fig. 4b). However, when an 85% gait, 15% stair partitioning of activities was considered (Fig. 4d), the predicted maximum damage location on the medial side also became consistent with the retrieval.

Quantitatively, the simulations predicted maximum total damage depths on the same order of magnitude as those measured from the retrieved insert (Table 1). The predicted maximum damage depths ranged from 0.7 to 2.7 mm. The predicted creep deformation was a substantial portion of the total damage. The 70–30 load split for gait and stair activities exhibited the deepest damage on the medial side, whereas the 50–50 load cases produced the deepest damage on the lateral side. Total damage area was greater for gait than for stair, while total damage volume was approximately 50% larger for stair than for gait. Smaller medial loads (50–50 split) decreased the damage volume in the medial compartment and increased damage volume in the lateral compartment such that the total damage volume was unaffected by load split.

Combining damage predictions from the two activities (85% gait, 15% stair) resulted in damage similar to the retrieved implant (Table 2). The predicted locations of maximum damage depth were the same as on the retrieved insert (Fig. 4d). Maximum damage depths for the retrieval were 0.7 mm medial and 0.8 mm lateral versus 0.8 and 0.9 mm for the simulation. The combined case predicted 112% of the total damage area on the retrieval, 114% medially and 108% laterally. The medial–lateral ratio for damage depth was 0.88 for the retrieval and 0.89 for the simulation while for damage area it was 1.38 for the retrieval and 1.47 for the simulation.

Table 2
Quantitative comparison between retrieval damage and simulation damage predicted by an activity partition of 85% gait, 15% stair with a 70–30 load split

Damage	Retrieval[a]			Simulation		
	Medial	Lateral	Total	Medial	Lateral	Total
Total depth (mm)	0.7	0.8	—	0.8	0.9	—
Area (mm^2)	422	305	727	483	329	812

[a] See Harman et al. (2001) for measurement details.

4. Discussion

This study used a novel combination of in vivo measurements, post-mortem observations, and computational tools to predict patient-specific damage in a total knee replacement. This approach allows researchers to "close the loop" on damage predictions by validating them against the tibial insert retrieved from the same patient whose in vivo kinematics were used as model inputs. Though the methodology requires a number of uncertain input parameters and modeling assumptions, integration of these approaches into a single cohesive framework leads to damage predictions that capture the important features of retrieval observations. With continuing refinements, this methodology may be useful for improving implant designs through virtual prototyping or predicting in vivo damage prior to clinical use.

Using knee kinematics from two activities (85% gait, 15% stair), it was possible to create bearing surface damage similar to the retrieved insert. The locations of maximum damage were the same (Fig. 4d), as were the ratios of damage between medial and lateral sides (Table 2). The maximum damage depth was greater for the simulations than the retrieval, in part because the model did not include creep relaxation. Similarly, predicted volumetric damage was 42–64 mm^3 per year, higher than published retrieval series. Lavernia et al. (2001) reported 31 mm^3 per year on autopsy retrieved devices of similar geometry, and Price et al. (2002) reported 8 mm^3 per year on fully conforming, mobile-bearing unicondylar knee replacements. It was somewhat surprising to find greater damage depth under the lateral condyle for both simulation and retrieval, but this was explained by the kinematics, where little translation of the lateral condyle focused damage in a smaller area. The medial condyle showed greater translations for both activities, creating greater damage areas, but shallower damage depths, both in simulation and in vivo.

Obviously, patients do not spend 15% of their weight-bearing cycles climbing stairs. It is reasonable to assume, however, that stair data provides an approximation to other activities involving the flexed knee under high load, such as sitting and rising from a chair or bed, using a toilet, entering and exiting a car, etc. The composite of these relatively less frequent, but highly demanding, activities could play a significant role in the damage experience of the prosthetic bearing.

The major difference between damage on the retrieved implant and the simulations was a modest amount of apparent damage at the periphery of the retrieved insert (Fig. 3b). Visual inspection of this region of the retrieval revealed negligible damage. One explanation of this apparent damage is that the implant had warped, upward at the tibial eminence, as has been observed on similar implants at autopsy (Jacobs et al., 2002). The inspection software registered the worn and unworn parts at the central eminence, so the periphery of the retrieval appeared lower, and consequently worn.

The dynamic contact modeling approach used in this study is extremely efficient computationally. Recent studies of knee wear simulator machines have used dynamic finite element analyses (FEA) to predict knee replacement kinematics and contact pressures simultaneously (Giddings et al., 2001; Godest et al., 2002). An advantage of dynamic FEA is that it also predicts internal stresses. However, a high computational price is paid for this benefit, with CPU times ranging from 1.4 days (Godest et al., 2002) to between 2.4 and 3.2 days (Giddings et al., 2001). Predicting kinematics alone requires 6–7 h of CPU time (Godest et al. 2002). To improve computational performance, a simplified dynamic FEA method that combines rigid body analysis with an elastic foundation contact model, similar to our approach, has recently been proposed (Halloran et al., 2003). By sacrificing internal stress calculations, this method can achieve CPU times comparable to those of the present study. Consequently, when only kinematics, contact forces, and/or contact pressures are of interest, hybrid rigid body/elastic contact approaches can provide faster alternatives to traditional dynamic FEA.

Despite its computational advantages, the current contact model formulation has limitations. It does not account for viscoelastic material properties (Waldman and Bryant, 1994, 1997), friction (Sathasivam and Walker, 1997), or how pressure applied at one location affects the displacement of other locations (Johnson, 1985). However, the most significant issue is the use of a linear material model. This model was chosen over a nonlinear model for two reasons. First, a linear model is more in line with the guiding concept of using models with previously published, well-established parameter values. Second, in recent simulations of a different knee implant using the same dynamic contact model, a linear model matched static contact pressure measurements better than did a nonlinear material model (Cripton, 1993) for 16 different loading conditions (loads of 750, 1500, 2250, and 3000 N and flexion angles of 0, 30, 60, and 90°; Fregly et al., 2003). The value of Young's modulus that reproduced the experimental data (400 MPa) was close to the value reported by Kurtz et al. (2002) as used here. Use of a nonlinear material model (Cripton, 1993) in the simulations produces more uniform contact pressures across a broader patch (Fig. 5). Thus, a nonlinear material model with well-established parameter values would produce broader damage predictions in the anterior–posterior direction, similar to the retrieval, but would not likely cause dramatic changes in the depth or distribution of predicted damage.

The spatially discrete nature of the predicted damage scars in the anterior–posterior direction, especially on the medial side, was due to variations in the input kinematics during a single motion cycle. Since the damage predictions integrate the combined effects of motion and loads on each element over the cycle, high loads during sliding at any point in the cycle will produce localized damage regions. Use of multiple experimental motion cycles or more accurate axial load inputs, if available, could produce more continuous anterior–posterior variation in predicted damage.

A constant 70–30 or 50–50 load split was used in the simulations as a simple approximation to the in vivo loads. It is tempting to use the external varus–valgus moment from gait analysis to define a variable load split throughout the gait or stair cycle. However, muscles play a significant role in balancing external moments at joints (Duda et al., 1997; Glitsch and Baumann, 1997; Lu et al., 1997, 1998), and the adduction moment resisted by tibiofemoral contact forces is likely much

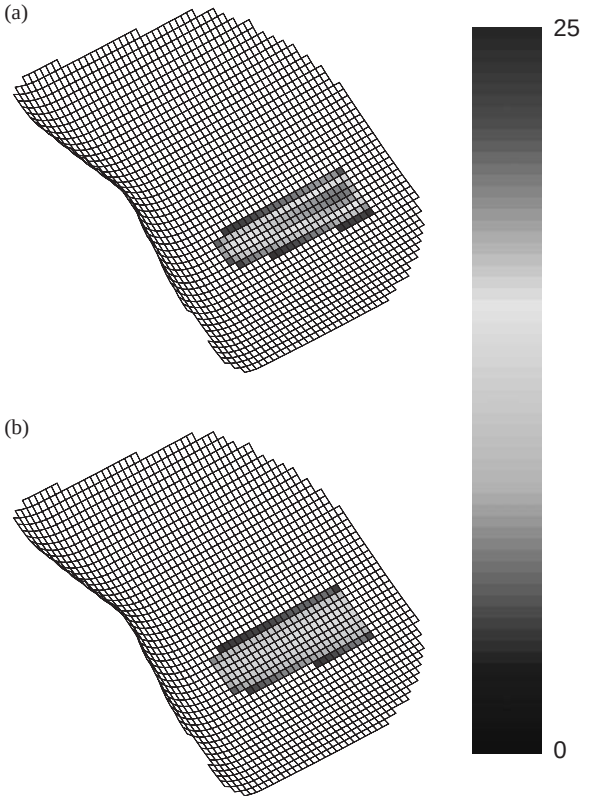

Fig. 5. Visualization of the static contact pressures predicted by the dynamic model for an axial load of 3 BW: (a) linear material model; and (b) nonlinear material model. Colorbar indicates pressure in MPa. The element grid is 50×50, the same as that used in the damage predictions.

smaller than the external knee adduction moment (Lu et al., 1997). Knowledge of muscle and ligament forces would be needed to calculate the variable contact moment from the external moment. For these reasons, a conservative 50–50 load split was used along with a 70–30 load split based on data in the literature (Johnson et al., 1981; Schipplein and Andriacchi, 1991; Hurwitz et al., 1998).

The damage computations required a number of input parameters that are not known with certainty. For pin-on-flat tribometer experiments using material pairs and loading conditions similar to joint replacements, measured values of the wear rate k for UHMWPE vary by orders of magnitude as a function of the average roughness R_a of the counterface. For R_a values between 18 and 72 nm, Fisher et al. (1994) reported k values ranging from 7.9×10^{-9} to 457×10^{-9} mm^3/Nm with a sudden increase in k at approximately $R_a = 50$ nm. This rapid increase is the motivation for highly polished and scratch-resistant femoral components. Wear rates have also been shown to be highly dependent on the extent of crossing motion (Bragdon et al., 1996; Muratoglu et al., 1999; Burroughs and Blanchet, 2001; Wang, 2001). For the implant and patient used in the present study, subsequent analyses performed by the authors suggest that no element on the tibial insert surface experienced bi-directional crossing motion greater than about 10° (Sawyer et al., 2004). Thus, adjusting the wear factor for crossing severity would have little effect on the damage predictions. By using accurate k values measured from pin-on-disk tribometer experiments, the wear performance of new femoral component materials could be predicted via computer simulation for specific knee designs prior to physical testing and clinical trials.

The precise number of load cycles of gait and stair was also unknown for the patient. Using an electronic pedometer, Schmalzried et al. (1998) measured the number of steps per day taken by hip and knee replacement patients. The average data extrapolated to 0.9 million cycles per year, ranging from 0.1 million to 3.2 million cycles per year. Since the wear per cycle δ_{Wear} is multiplied by the number of cycles per year N, the wear predictions can vary substantially based on the patient's assumed activity level.

Finally, simulations of a single cycle of gait and/or stair were used to develop all damage predictions, with no changes in surface geometry due to repeated loading taken into account. In many mechanisms, accurate wear prediction requires accounting for the coupled evolution of wear, kinematics, and load (Blanchet, 1997; Sawyer et al., 2003; Dickrell et al., 2003). To determine the number of cycles that a single simulation could be extrapolated for wear prediction before changes in surface geometry were required, Dickrell et al., 2003 used a combined experimental, analytical, and computer simulation approach. They found that if loads and surface geometry change little, extrapolation of a single simulation over a large number of cycles is reasonable. For patients with knee replacements, the loads during daily activities are relatively constant, and the damage depths are orders of magnitude smaller than the radii of curvature of the components. Thus, the effect of form changes on subsequent kinematics, slip velocities, slip distances, and contact pressures is expected to be low, making the system weakly coupled and extrapolation errors small.

This study has presented a novel approach for performing computational wear predictions of total knee replacements. Despite a large number of simplifying assumptions, the methodology produces damage predictions reasonably consistent with retrieval observations. Using in vivo kinematic data from fluoroscopy to drive a dynamic contact model, damage on differential elements of the tibial insert surface can be predicted. Modeling knee simulator machines, where the load and kinematic inputs are better defined, will provide a valuable avenue for refining the methodology and validating its predictions. Eventually, it may be possible to use similar computational tools to augment traditional in vitro mechanical testing, predict damage performance of novel implants or materials in early

clinical trials, and evaluate systematically the effects of variable surgical positioning on subsequent implant performance.

Acknowledgements

This study was supported by new faculty start-up funds from the University of Florida and by The Biomotion Foundation of West Palm Beach, Florida. We thank Stryker Howmedica Osteonics for providing the CAD models used in the simulations, Yanhong Bei for assistance with elastic contact model development, and Matt Hamilton for assistance with computational wear model development.

Appendix A

List of web sites for commercial implant materials intended to reduce mild wear:

Scratch-resistant femoral materials

Oxinium™ oxidized zirconium (Smith & Nephew)
http://www.oxinium.com/default.html

Zirconia ceramic (Kinamed)
http://www.carbojet.com/gem.html

Crosslinked polyethylene

Crossfire™ (Stryker Howmedica Osteonics)
http://www.stryker.com/jointreplacements/sites/crossfire

Durasul™ (Zimmer)
http://www.centerpulseorthopedics.com/durasul/index.html

Longevity™ (Zimmer)
http://www.zimmer.com/ctl?op=global&action=1&id=31&template=MP

Marathon™ (DePuy)
http://www.jnjgateway.com/home.jhtml?loc=USENG&page=viewContent&contentId=fc0de00100000498

References

An, K.N., Himenso, S., Tsumura, H., Kawai, T., Chao, E.Y.S., 1990. Pressure distribution on articular surfaces: application to joint stability analysis. Journal of Biomechanics 23, 1013–1020.

Archard, J.F., Hirst, W., 1956. The wear of metals under unlubricated conditions. Proceedings of the Royal Society A 236, 397–410.

Banks, S.A., 1992. Model based 3D kinematic estimation from 2D perspective silhouettes: application with total knee prostheses. Ph.D. Dissertation, Massachusetts Institute of Technology, Cambridge, MA.

Banks, S.A., Hodge, W.A., 1996. Accurate measurement of three-dimensional knee replacement kinematics using single-plane fluoroscopy. IEEE Transactions on Biomedical Engineering 43, 638–649.

Banks, S.A., Markovich, G.D., Hodge, W.A, 1997a. In vivo kinematics of cruciate-retaining and substituting knee arthroplasties. Journal of Arthroplasty 12, 297–304.

Banks, S.A., Markovich, G.D., Hodge, W.A., 1997b. The mechanics of knee replacements during gait: in vivo fluoroscopic analysis of two designs. American Journal of Knee Surgery 10, 261–267.

Banks, S.A., Otis, J.C., Backus, S.I., Furman, G.L., Haas, S.B., 2000. Function of total knee replacements during activities of daily living. In: Proceedings of the 67th Annual Meeting of the American Academy of Orthopaedic Surgeons, Orlando, FL, March.

Bartel, D.L., Rawlinson, J.J., Burstein, A.H., Ranawat, C.S., Flynn, W.F., 1995. Stresses in polyethylene components of contemporary total knee replacements. Clinical Orthopaedics and Related Research 317, 76–82.

Blanchet, T.A., 1997. The interaction of wear and dynamics of a simple mechanism. Journal of Tribology 119, 597–599.

Blankevoort, L., Kuiper, J.H., Huiskes, R., Grootenboer, H.J., 1991. Articular contact in a three-dimensional model of the knee. Journal of Biomechanics 24, 1019–1031.

Blunn, G.W., Walker, P.S., Joshi, A., Hardinge, K., 1991. The dominance of cyclic sliding in producing wear in total knee replacements. Clinical Orthopaedics and Related Research 273, 253–260.

Bragdon, C.R., O'Conner, D.O., Lowenstein, J.D., Jasty, M., Syniuta, W.D., 1996. The importance of multidirectional motion on the wear of polyethylene. IMechE Part H: Journal of Engineering in Medicine 210, 157–165.

Burroughs, B.R., Blanchet, T.A., 2001. Factors affecting the wear of irradiated UHMWPE. Tribology Transactions 44, 215–223.

Cadambi, A., Engh, G.A., Dwyer, K.A., Vinh, T.N., 1994. Osteolysis of the distal femur after total knee arthroplasty. Journal of Arthoplasty 9, 579–594.

Cripton, P.A., 1993. Compressive characterization of ultra-high molecular weight polyethylene with applications to contact stress analysis of total knee replacements. Master of Science Thesis, Queen's University, Kingston, Ontario.

Dickrell, D.J., Dooner, D.B., Sawyer, W.G., 2003. The evolution of geometry for a wearing circular cam: analytical and computer simulation with comparison to experiment. Journal of Tribology 125, 187–192.

Duda, G.N., Schneider, E., Chao, E.Y.S., 1997. Internal forces and moments in the femur during walking. Journal of Biomechanics 30, 933–941.

Ewald, F.C., 1989. The knee society total knee arthroplasty roentgenographic evaluation and scoring system. Clinical Orthopaedics and Related Research 248, 9–12.

Ezzet, K.A., Garcia, R., Barrack, R.L., 1995. Effect of component fixation method on osteolysis in total knee arthroplasty. Clinical Orthopaedics and Related Research 321, 86–91.

Fisher, J., Dowson, D., Hamdzah, H., Lee, H.L., 1994. The effect of sliding velocity on the friction and wear of UHMWPE for use in total artificial joints. Wear 175, 219–225.

Fregly, B.J., Bei, Y., Sylvester, M.E., 2003. Experimental evaluation of an elastic foundation model to predict contact pressures in knee replacements. Journal of Biomechanics 36, 1659–1668.

Giddings, V.L., Kurtz, S.M., Edidin, A.A., 2001. Total knee replacement polyethylene stresses during loading in a knee simulator. Journal of Tribology 123, 842–847.

Glitsch, U., Baumann, W., 1997. The three-dimensional determination of internal loads in the lower extremity. Journal of Biomechanics 30, 1123–1131.

Godest, A.C., Meaugonin, M., Haug, E., Taylor, M., Gregson, P.J., 2002. Simulation of a knee joint replacement during a gait cycle using explicit finite element analysis. Journal of Biomechanics 35, 267–276.

Halloran, J.P., Easley, S.K., Penmetsa, J., Laz, P.J., Petrella, A.J., Rullkoetter, P.J., 2003. Efficient dynamic finite element rigid body analysis of TJR. In: Proceedings of the 2003 ASME Summer Bioengineering Conference, Key Biscayne, FL, June 25–29.

Harman, M.K., Banks, S.A., Hodge, W.A., 2001. Polyethylene damage and knee kinematics after total knee arthroplasty. Clinical Orthopaedics and Related Research 392, 383–393.

Heimke, G., Leyen, S., Willmann, G., 2002. Knee arthroplasty: recently developed ceramics offer new solutions. Biomaterials 23, 1539–1551.

Hurwitz, D.E., Sumer, D.R., Andriacchi, T.P., Sugar, D.A., 1998. Dynamic knee loads during gait predict proximal tibial bone distribution. Journal of Biomechanics 31, 423–430.

Insall, J.N., Dorr, L.D., Scott, R.D., Scott, W.N., 1989. Rationale of the knee society clinical rating system. Clinical Orthopaedics and Related Research 248, 13–14.

Jacobs, J.J., Shanbhag, A., Glant, T.T., Black, J., Galante, J.O., 1994. Wear debris in total joint replacements. Journal of the American Academy of Orthopaedic Surgeons 2, 212–220.

Jacobs, J.J., Surace, M.F., Berzins, A., Urban, R.M., Berger, R.A., Natarajan, R.N., Andriacchi, T.P., Galante, J.O., 2002. Backsided tibial polyethylene wear and osteolysis in modular tibial components. In: Proceedings of the Knee Society, Dallas, TX, February 16.

Johnson, F., Scarrow, P., Waugh, W., 1981. Assessments of loads in the knee joint. Medical and Biological Engineering and Computing 19, 237–243.

Johnson, K.L., 1985. Contact Mechanics. Cambridge University Press, Cambridge.

Kurtz, S.M., Jewett, C.W., Bergström, J.S., Foulds, J.R., Edidin, A.A., 2002. Miniature specimen shear punch test for UHMWPE used in total joint replacements. Biomatierals 23, 1907–1919.

Lavernia, C.J., Sierra, R.J., Hungerford, D.S., Krackow, K., 2001. Activity level and wear in total knee arthroplasty: a study of autopsy retrieved specimens. Journal of Arthroplasty 16, 446–453.

Lee, K.Y., Pienkowski, D., 1998. Compressive creep characteristics of extruded ultrahigh-molecular-weight polyethylene. Journal of Biomedical Materials Research 39, 261–265.

Lewis, G., 1997. Polyethylene wear in total hip and knee arthroplasties. Journal of Biomedical Materials Research (Applied Biomaterials) 38, 55–75.

Li, G., Sakamoto, M., Chao, E.Y.S., 1997. A comparison of different methods in predicting static pressure distribution in articulating joints. Journal of Biomechanics 30, 635–638.

Li, S., Burstein, A.H., 1994. Ultra-high molecular weight polyethylene: the material and its use in total joint implants. Journal of Bone and Joint Surgery 76-A, 1080–1090.

Lu, T.-W., Taylor, S.J.G., O'Connor, J.J., Walker, P.S., 1997. Influence of muscle activity on the forces in the femur: an in vivo study. Journal of Biomechanics 30, 1101–1106.

Lu, T.-W., O'Connor, J.J., Taylor, S.J.G., Walker, P.S., 1998. Validation of a lower limb model with in vivo femoral forces telemetered from two subjects. Journal of Biomechanics 31, 63–69.

McKellop, H., Shen, F.W., Lu, B., Campbell, P., Salovey, R., 1999. Development of an extremely wear-resistant ultra high molecular weight polyethylene for total hip replacements. Journal of Orthopaedic Research 17, 157–167.

Muratoglu, O.K., Bragdon, C.R., O'Conner, D.O., Jasty, M., Harris, W.H., Gul, R., McGarry, F., 1999. Unified wear model for highly crosslinked ultra-high molecular weight polyethylenes (UHMWPE). Biomaterials 20, 1463–1470.

Peters, P.C., Engh, G.A., Dwyer, K.A., Vinh, T.N., 1992. Osteolysis after total knee arthroplasty without cement. Journal of Bone and Joint Surgery 74-A, 864–876.

Price, A., Short, A., Kellett, C., Rees, J., Pandit, H., Dodd, C., McLardy-Smith, P., Gundle, R., Murray, D., 2002. Ten-year in vivo wear measurement of a fully congruent mobile-bearing unicompartmental knee arthroplasty. In: Proceedings of the 15th Annual Symposium of the International Society for Technology in Arthroplasty, Oxford, England, September 26–28.

Sathasivam, S., Walker, P.S., 1997. Computer model with surface friction for the prediction of total knee kinematics. Journal of Biomechanics 30, 177–184.

Sathasivam, S., Walker, P.S., 1998. Computer model to predict subsurface damage in tibial inserts of total knees. Journal of Orthopaedic Research 16, 564–571.

Sawyer, W.G., Diaz, K.I., Hamilton, M.A., Micklos, B., 2003. Evaluation of a model for the evolution of wear in a scotch-yoke mechanism. Journal of Tribology 125, 678–681.

Sawyer, W.G., Hamilton, M.A., Succec, M.C., Fregly, B.J., Banks, S.A., 2004. Quantifying multidirectional sliding motions in total knee replacements. Journal of Tribology, in press.

Schipplein, O.D., Andriacchi, T.P., 1991. Interaction between active and passive knee stabilizers during level walking. Journal of Orthopaedic Research 9, 113–119.

Schmalzried, T.P., Szuszczewicz, E.S., Northfield, M.R., Akizuki, K.H., Frankel, R.E., Belcher, G., Amstutz, H.C., 1998. Quantitative assessment of walking activity after total hip or knee replacement. Journal of Bone and Joint Surgery 80-A, 54–59.

Sharkey, P.F., Hozack, W.J., Rothman, R.H., Shastri, S., Jacoby, S.M., 2002. Why are knee replacements failing today? In: Proceedings of the Knee Society, Dallas, TX, February 16.

Taylor, S.J.G., Walker, P.S., 2001. Force and moments telemetered from two distal femoral replacements during various activities. Journal of Biomechanics 34, 839–848.

Taylor, S.J.G., Walker, P.S., Perry, J.S., Cannon, S.R., Woledge, R., 1998. The forces in the distal femur and the knee during walking and other activities measured by telemetry. Journal of Arthroplasty 13, 428–437.

Waldman, S.D., Bryant, J.T., 1994. Compressive stress relaxation behavior of irradiated ultra-high molecular weight polyethylene at 37°C. Journal of Applied Biomaterials 5, 333–338.

Waldman, S.D., Bryant, J.T., 1997. Dynamic contact stress and rolling resistance model for total knee arthroplasties. Journal of Biomechanical Engineering 119, 254–260.

Walker, P.S., Blunn, G.W., Lilley, P.A., 1996. Wear testing of materials and surfaces for total knee replacements. Journal of Biomedical Materials Research 33, 159–175.

Wang, A., 2001. A unified theory of wear for ultra-high molecular weight polyethylene in multi-directional sliding. Wear 248, 38–47.

Williams, I.R., Mayor, M.B., Collier, J.P., 1998. The impact of sterilization method on wear in knee arthroplasty. Clinical Orthopaedics and Related Research 356, 170–180.

Wimmer, M.A., Andriacchi, T.P., 1997. Tractive forces during rolling motion of the knee: implications for wear in total knee replacement. Journal of Biomechanics 30, 131–137.

Wimmer, M.A., Andriacchi, T.P., Natarajan, R.N., Loos, J., Karlhuber, M., Petermann, J., Schneider, E., Rosenberg, A.G., 1998. A striated pattern of wear in ultrahigh-molecular-weight polyethylene components of miller-galante knee arthoplasty. Journal of Arthroplasty 13, 8–16.

Wroblewski, B.M., Siney, P.D., Fleming, P.A., 1999. Low friction arthroplasty of the hip using alumina ceramic and crosslinked polyethylene—a ten-year follow-up report. Journal of Bone and Joint Surgery 81-B, 54–55.